

## Propagation Characteristics of Liquid Core Fibers, Part II: Interference and Ellipticity Induced Oscillations

SUSANA A. PLANAS, ERIK J. BOCHOVE and RAMAMANT SRIVASTAVA

Instituto de Física, Universidade Estadual de Campinas, Caixa Postal 6165, Campinas, 13100, SP, Brasil

Recebido em 19 de outubro de 1984

**Abstract** We have observed two kinds of oscillation in the intensity transmitted by liquid-core fibers as a function of temperature. The faster oscillations are interpreted as due to interference between various mode groups of the circular fiber, whereas a slower modulation with periods an order of magnitude larger are caused by beating among modes belonging to the same mode groups which are non-degenerate due to core ellipticity. A simple theory is shown to yield good agreement with our data and has been applied to make high-precision non-destructive measurements of core radius and core ellipticity along the fiber length.

### 1. INTRODUCTION

Optical fibers support a finite number of guided modes with discrete propagation constants at any given wavelength of the light radiation. Simplified theoretical expressions<sup>1</sup> have been derived for mode parameters in the case of fibers with circular symmetry and a small difference between the refractive indices of core and cladding. It has been found that the modes are approximately linearly polarized (called LP modes) and their normalized propagation constants can be expressed as a function of the normalized frequency  $v$  of the fibers given by

$$v = \frac{2\pi a}{\lambda} (n_c^2 - n^2)^{1/2} \quad (1)$$

where  $\lambda$  is the radiation wavelength in vacuo,  $a$  is the fiber core radius and  $n_c$  and  $n$  are the refractive index of the core and cladding respectively. The propagation constant  $\beta$  of any guided mode is restricted to the range  $n k < \beta < n_c k$  where  $k = 2\pi/\lambda$ . Gloge<sup>1</sup> has calculated the  $\beta(v)$  curves by solution of characteristic equation for low-order modes and determined the cutoff  $v$ -values ( $v_c$ ) for these modes.

The number of guided modes depend on the  $v$ -value of the fiber. As  $v$  increases, the number of guided modes will increase. In glass fibers, a way to vary  $v$  is to employ a wavelength tunable source of radi-

ation. Singlemode optical fibers have been characterized by the cutoff wavelength of the  $LP_{1,1}$  mode using this technique<sup>2</sup>. If liquid is used as the core material,  $v$  can also be varied by heating the fiber exploiting the high temperature dependence of the liquid refractive index  $n_c$ . This technique has been used in our laboratory to study mode cut-offs<sup>3</sup>, and the results were in good agreement with the theoretical values<sup>1</sup>. We have also shown how the core-radius can be obtained from this kind of study.

In this work, the birefringence induced by a small core ellipticity is detected by the presence of oscillations in the pattern of the transmitted intensity vs. temperature. An envelope of period about  $0.5^\circ\text{C}$ , modulates another set of oscillations of period  $0.05^\circ\text{C}$ . The lower period corresponds to interference between different LP mode groups and the envelope corresponds to interference between degenerate modes of the same mode group. The experimental data are discussed based in the two mechanisms of interference and fitting the data to the theoretical expressions we derived values for the core radius and its ellipticity.

This technique of geometrical characterization is more accurate than the crossed polarizers technique<sup>4</sup> and can be easily applied to high precision measurements of core radius and ellipticity of hollow fibers, with the advantage of being non-destructive.

## 2. THEORY

As mentioned earlier, weakly guiding mode theory<sup>5</sup> gives approximate analytical solutions for the mode parameters. In our work<sup>3</sup> we have summarized the basic concepts of this theory. Here we consider the basic equations needed to describe the oscillatory behaviour of the intensity pattern using relatively simple expressions for interference between two or three guided modes and calculate the frequency of the oscillations in terms of the fiber mode parameters. A brief discussion of birefringence in optics precedes the derivation of expressions for the period of the oscillations involving beating between the components belonging to different polarizations of the same LP mode group.

### A. Basic Equations of the Beat Phenomena

Consider the case of many modes being propagated by the fiber, a length  $L$  of which has been placed in a furnace. The field configura-

ation  $\vec{E}(\vec{\rho}, L)$  that results, neglecting mode coupling effects at the fiber output is

$$\vec{E}(\vec{\rho}, L) = \sum_n \frac{\alpha_n \vec{e}_n(\rho)}{N_n} g_n \exp. [\beta_n L + \phi_n] - \frac{1}{2} \alpha_n L \quad (2)$$

where  $\alpha_n$  is the temperature dependent power loss coefficient of the  $n^{\text{th}}$  mode inside the furnace;  $\beta_n$  is its temperature dependent propagation constant inside the furnace,  $\vec{\rho}$  is the radial vector;  $\phi_n$  and  $g_n$  are respectively the parts of the phase and a loss factor which are both independent of the furnace temperature and dependent on the length of fiber outside the furnace, and  $N_n$  is a normalization parameter

$$N_n = \left[ \int_{\infty} e_n^2 d^2 \rho \right]^{1/2} \quad (3)$$

The intensity at a certain distance from the fibers output is given by

$$|\vec{E}'(\vec{\rho}, L)|^2 = \sum_n \alpha_n^2 g_n^2 e_n'(\vec{\rho}) e^{-\alpha_n L} / N_n^2 \quad (4)$$

$$+ \sum_{n \neq m} \alpha_n \alpha_m g_n g_m \times \frac{\vec{e}_n'(\vec{\rho}) \vec{e}_m'(\vec{\rho})}{N_n N_m} \exp\{i [(\beta_n - \beta_m) L + \phi_n - \phi_m] - \frac{1}{2} (\alpha_n + \alpha_m) L\}$$

The fields  $e_n'(\rho)$  are the fiber mode fields  $\vec{e}_n(\vec{\rho})$  where the prime indicates a possible integral transform due to radiation to the far-field location in the detector.

The total power transmitted through an area  $s$  measured by the detector which is placed at a small distance from the output end of the fiber is given by

$$P_d = \int_s |\vec{E}'|^2 ds = \sum_n |\alpha_n|^2 g_n^2 \exp. (-\alpha_n L) \int_s \frac{\vec{e}_n'^2(\vec{\rho}) ds}{N_n^2} + \sum_{n \neq m} \alpha_n \alpha_m g_n g_m \times \cos [(\beta_n - \beta_m)L + \phi_n - \phi_m] \exp \left[ \frac{-(\phi_n + \phi_m)L}{2} \right] \int_s \frac{\vec{e}_n'(\vec{\rho}) e_m'(\rho) ds}{N_n N_m} \quad (5)$$

This can be written as a sum over the power contributed by individual modes plus interference terms between mode pairs, in the form

$$P_d = \sum_n p_n f_n e^{-\alpha_n(T)L} + \sum_{m \neq n} \sqrt{p_n p_m} f_{nm} e^{-\frac{1}{2} [\alpha_n(T) + \alpha_m(T)]L} \times \cos [(\beta_n(T) - \beta_m(T))L + \phi_n - \phi_m] \quad (6)$$

where the symbols used are:

$P_n$  = output power in the  $n^{\text{th}}$  fiber mode omitting loss in the furnace.

$f_n$  = fraction of light in the  $n^{\text{th}}$  mode which is detected.

$f_{nm}$  = intermode overlap integral at the detecting surface, given by

$$f_{nm} = \frac{\int_{\vec{d}} \vec{e}_n'(\vec{\rho}) \cdot \vec{e}_m'(\vec{\rho}) ds}{\left[ \int \vec{e}_n'^2(\vec{\rho}) ds \right]^{1/2} \left[ \int \vec{e}_m'^2(\vec{\rho}) ds \right]^{1/2}} \quad (7)$$

where the integral in the numerator is performed over that part of the detector surface which is exposed to the light, and those integrals in the denominator are over the entire plane of the detector surface.

In order to observe interference it is necessary that  $f_{nm} \neq 0$ . If  $n \neq m$ , by mode orthogonality we have  $f_{nm} = 0$  if the detector is placed so as to detect all the emerging light. It is therefore necessary to enhance the interference by truncating the field over the detector surface by means of a spatial filter.

Eq. (6) describes all temperature dependence of losses and interference through the temperature dependence of  $\alpha_n$  and  $\beta_m$  respectively. In order to describe the mode cutoff effect as a function of temperature, no more detailed theoretical analysis is needed, except the observation that the cutoff of the  $n^{\text{th}}$  mode is defined as the point where  $\exp(-\alpha_n L)$  vanishes. On the other hand, to explain the mode interference, exact expressions for the relevant  $\beta_n(T)$  are needed. These functions depend on the modal properties of the fiber, as well as on the temperature dependence of the refractive index of the liquid core. Measurements of the interference pattern of a relatively small number of modes (two or three) would, in principle, allow for a means of studying propagation properties of fiber lengths equal to that over which its temperature is varied.

## B. Interference of two modes

Joining terms which are irrelevant to the present discussion, eq. (6) takes the form

$$P_d^{(2)} = C_0 + C_{12} \cos [(\beta_1 - \beta_2)L + \phi_1 - \phi_2] \quad (8)$$

showing explicitly only the interference term. Considering the temperature as variable, the frequency of oscillation is defined by

$$\nu_{12}(T) = \frac{1}{2\pi} \frac{d}{dT} (\beta_1 - \beta_2)L \quad (9)$$

In section D we derive an expression for  $\nu_{12}(T)$  in the case interference between two LP mode groups of the circular fiber.

### C. Interference of three modes

For the case of three modes, showing again explicitly only the interference terms, eq. (8) takes the form

$$P_d^{(3)} = C_0 + C_{12} \cos [(\beta_1 - \beta_2)L + (\phi_1 - \phi_2)] + C_{13} \cos [(\beta_1 - \beta_3)L + \phi_1 - \phi_3] + C_{23} \cos [(\beta_2 - \beta_3)L + \phi_2 - \phi_3] \quad (10)$$

This rather complicated expression fortunately simplifies to a form which is consistent with the data, if certain relations among the constants  $C_{nm}$  and  $\beta_n$  are assumed. Thus, take  $\beta_1 \approx \beta_2$  and  $C_{13} = C_{23}$ . The first condition is satisfied when modes 1 and 2 belong to the same LP mode group. The second condition requires equality of powers and overlap fractions,  $p_1 = p_2$  and  $f_{13} = f_{23}$ , which is also likely to be met when the modes 1 and 2 belong to the same LP group. Eq. (10) then becomes

$$P_d^{(3)} \approx C_0 + C_{12} \cos [(\beta_1 - \beta_2)L + \phi_1 - \phi_2] + 2C_{13} \cos \left[ \frac{1}{2} (\beta_1 - \beta_2)L + \frac{1}{2} (\phi_1 + \phi_2) \right] \times \cos [(\beta_3 - \beta_1)L - \frac{1}{2} (\phi_1 + \phi_2) + \phi_3] \quad (11)$$

The third term in this equation is the most important for the purpose of this work. It oscillates at the frequency

$$\nu_{13}(T) = \frac{1}{2\pi} \frac{d}{dT} (\beta_3 - \beta_1)L \quad (12)$$

while its amplitude is modulated at the lower frequency  $\nu'_{12}(T) \ll \nu_{13}(T)$

$$\nu'_{12}(T) = \frac{1}{4\pi} \frac{d}{dT} (\beta_1 - \beta_2)L \quad (13)$$

The second term in eq. (11) results in a *bending* of the third term. The

oscillatory behavior predicted by eqs. (12) and (13) was observed in the experiments.

Now we can derive explicit expressions for the beat periods in terms of fiber mode parameters. It is assumed that the smaller period is due to interference between two different *LP* mode groups and the larger one is due to birefringence induced by core ellipticity.

#### D. Beating between different *LP* mode groups

When the two modes that interfere are those of the circular fiber, the beat period due to the difference in  $\beta$ 's corresponding to different *LP* modes can be calculated from Gloge's theory. Accordingly we find it convenient to use in place of  $\beta$  the parameter  $b$  defined by<sup>1</sup>

$$b = [(\beta/nk) - 1]/\Delta ; A = (nc - n)/n \quad (14)$$

The mode parameters are given in terms of  $b$  by

$$w = v\sqrt{b} \quad (15)$$

and

$$u = v\sqrt{1-b} \quad (16)$$

Differentiating eq. (14) with respect to the temperature  $T$ , and using eqs (15) and (16), we obtain

$$\frac{d\beta}{dT} = nk \left( b + \frac{1}{2} v \frac{\partial b}{\partial v} \right) \frac{d\Delta}{dT} \quad (17)$$

The derivative  $\partial b/\partial v$  may be eliminated by means of the relation

$$\frac{a}{\partial v} (bv) = b + 2\kappa(1-b) \quad (18)$$

where

$$\kappa = K_{\ell}^2(w)/K_{\ell-1}(w)K_{\ell+1}(w)$$

Using Gloge's eq. (29) for  $P_c/P_t$ , the ratio of power guided by the core to total power, eq. (17) becomes

$$\frac{d\beta}{dT} = k \frac{dn_c}{dT} \frac{P_c}{P_T} \quad (19)$$

By eq. (12), the period of the beats between two different *LP* modes having the values  $P_{c_2}/P_{t_2}$  and  $P_{c_1}/P_{t_1}$  respectively for the fraction of power in the mode to the total power, is given by

$$P_{13} = \lambda/L \frac{dn_c}{dT} \left[ \frac{P_{c3}}{P_{t3}} - \frac{P_{c1}}{P_{t1}} \right] \quad (20)$$

The behavior of eq. (20) for various mode pairs is illustrated in fig.6. Each curve shown is discontinued at the cut-off point of one of the members of the corresponding pair, except for the pair  $LP_{21}$  and  $LP_{02}$ , which has the same cut-off. Far from cut-off,  $P_c/P_t$  approaches unity for all modes, so that accordingly to eq. (20) the beat period approaches infinity. Close to cut off, the ratio  $P_c/P_t$  is a minimum for the mode in question, resulting in the smallest value for the beat period.

### E. Geometry Induced Birefringence

The origins of birefringence are twofold: 1) an ellipticity in the core; 2) the presence of an asymmetrical residual stress distribution in the case of solid core fibers. In the case of liquid core fibers the last factor is absent.

A linearly polarized light beam incident in the direction of the fibre axis can be considered to be split into two wave components polarized along the preferred axes of symmetry denoted  $x, y$  respectively. Nominally circular core single mode fibers are slightly elliptical and consequently possess two non-degenerate orthogonal modes of propagation constants,  $\beta_x$  and  $\beta_y$ . On emerging from the end face of the fiber, these modes have a phase difference  $\delta = (\beta_x - \beta_y)L$ , so that in this birefringent model, the light will experience two guide refractive indexes and the phase retardation is temperature dependence. The birefringence induced by small ellipticity<sup>5</sup> for  $R=0$  is given by

$$\beta_x - \beta_y = \frac{\epsilon^2 (2\Delta)^{3/2}}{8a} \frac{u^2 w^2}{v^3} \left[ 1 + \frac{uK_0^2(w) J_2(u)}{K_1^2(w) J_1(u)} \right]_{l=0} \quad (21)$$

where  $e$  is the core excentricity given by

$$e = \left[ 1 - \left( \frac{\text{minor axis}}{\text{major axis}} \right)^2 \right]^{1/2}$$

For  $l > 0$ , even and odd parity modes exist corresponding to  $\cos(l\phi)$  and  $\sin(l\phi)$  solutions. The corresponding propagation constants

are denoted  $\beta_e$  and  $\beta_0$  respectively. The difference  $\beta_e - \beta_0$  for the slightly elliptical fiber can be calculated from perturbation theory, yielding for  $l=1$

$$\beta_e - \beta_0 = \frac{e^2}{4a} \sqrt{2\Delta} \frac{u^2}{v} \kappa, \quad l=1 \quad (22)$$

In the multimode case, the importance of the eccentricity effects relative to  $\beta$  splitting of exact  $\text{EH}_{l-1,m}$  and  $\text{HE}_{l+1,m}$  modes belonging to the  $\text{LP}_{lm}$  group, may be described by the parameter  $\Lambda$  defined by Snyder and Young<sup>5</sup> as

$$\Lambda = \frac{\beta_e - \beta_0}{\beta_{\text{EH}} - \beta_{\text{HE}}} \quad (23)$$

If the eccentricity parameter is  $|\Lambda| \ll 1$ , the modes of the elliptical fibre are the true EH, HE modes of the circular symmetric wave-guide, while if  $|\Lambda| \gg 1$ , the modes are the LP modes (uniformly polarized).

#### F. Modulation Induced by Core Ellipticity

The period of slow modulation  $P_D$  predicted when three modes interfere, is given by eq. (13) and can be written as

$$P_D = 4\pi / \left[ L \frac{d}{dT} (\beta_1 - \beta_2) \right] \quad (24)$$

When the birefringence is induced by a small ellipticity in the core and  $|\Lambda| \gg 1$ , the observed beating occurs between the two polarizations of the same LP mode.

In the particular case  $l=1$ , differentiation of eq. (22) with respect to temperature yields

$$\frac{d}{dT} (\beta_e - \beta_0) = \frac{e^2 \lambda}{8\pi a^2 n} \left[ 2u \frac{\partial u}{\partial T} \kappa_1 + u^2 \frac{\partial \kappa}{\partial T} \right] \quad (25)$$

where

$$\frac{\partial u}{\partial T} = \frac{v}{n2\Delta\sqrt{1-b}} \frac{1}{\partial T} \left[ 1 - \frac{P_c}{P_T} \right] \quad (26j)$$

$$\frac{\partial \kappa_1}{\partial T} = \frac{v}{\sqrt{b} 2\Delta n} \frac{\partial n_c}{\partial T} \frac{P_c}{P} \kappa_1 A \quad (27)$$

and

$$A = \left[ -2 \frac{K_0}{K_1} + \frac{K_1}{K_0} + \frac{K_1}{K_2} \right] \quad (28)$$

Substituting in eqs. (26) and (27) in eq. (25) gives



$$\frac{\partial}{\partial T} (\beta_e - \beta_0) = \frac{e^2 \pi \kappa_1}{\lambda} \frac{\partial n_e}{\partial T} \left\{ 1 - \frac{P_c}{P_T} \left[ 1 - \frac{v^2 A}{2w} \right] \right\} \quad (29)$$

Therefore, eq. (24) becomes

$$P_D = 4\lambda / \left\{ L e^2 \kappa_1 \frac{\partial n_e}{\partial T} \left[ 1 - \frac{P_c}{P_T} \left( 1 - \frac{v^2 A}{2w} \right) \right] \right\} \quad (30)$$

This equation gives the period of birefringence in  $LP_{11}$  mode induced by core ellipticity and was used to calculate the low frequency period observed in the experiment.

### 3. EXPERIMENTAL

The experimental arrangement used to measure the transmitted light is given in fig.1 and described in detail in Ref.3. The heating rate, below  $0.5^\circ\text{C}/\text{min}$  was sufficiently slow so that the system could be maintained in quasi-thermal equilibrium. In most cases, transmitted and scattered intensities were measured simultaneously. Measurements were done during the heating as well as during the cooling process in order to check for the reproducibility of the results.

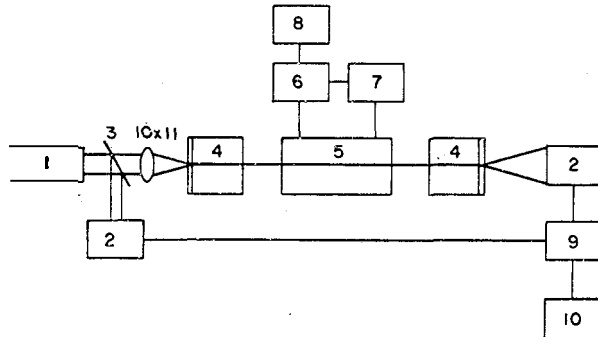


Fig.1 - Block diagram of the experimental arrangement: 1 - HeNe Laser; 2 - Power Meter; 3 - Beam Splitter; 4 - Liquid Cell; 5 - Furnace; 6 - Thermocouple; 7 - Temperature Controller; 8 - Digital Voltmeter; 9 - Voltage Divider; 10 - Chart Recorder; 11 - Fiber.

Fig. 2 shows the variation of the transmitted Intensity of fiber D as its temperature was varied. The fiber has liquid paraffin as the core material ( $n_D(20^\circ\text{C}) = 1.4640$ ) with  $5.5 \mu\text{m}$  radius. As the temperature is increased, besides mode cut-offs marked by a sudden drop in the Intensity, periodic oscillations occur in the region of  $25$  to  $29^\circ\text{C}$ . By visual observation of the near field pattern and the fact that the oscillations disappear at cut-off, one could verify that one of the interfering modes belongs to the  $LP_{02}$  mode group. The other interfering mode group is expected to be either the  $LP_{11}$  or  $LP_{01}$ . As shown below, only the interference between  $LP_{11}$  and  $LP_{02}$  mode groups can explain the observed data.

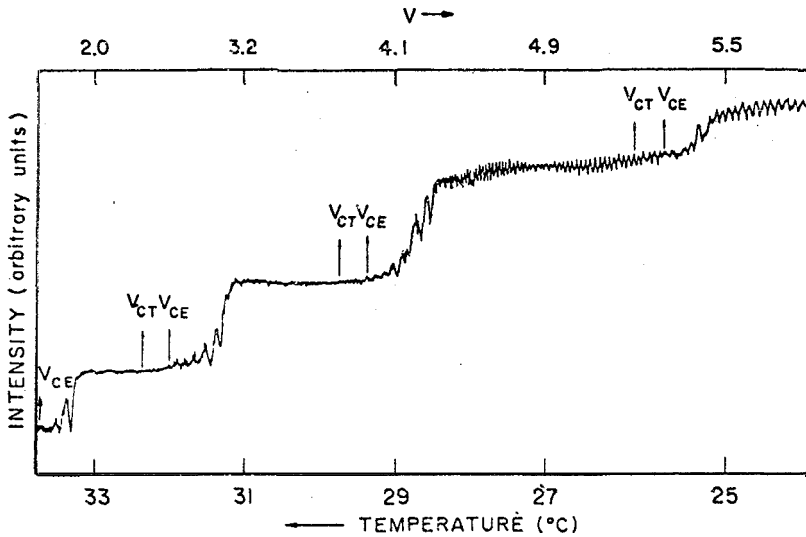


Fig.2 - Transmitted Intensity of fiber D as a function of temperature and  $v$ -value.  $v_{CE}$  and  $v_{CT}$  are the experimental and theoretical mode cut off  $v$ -values, respectively.

Figure 3 shows the variations in the transmitted intensity when this fiber A was heated (heavy paraffin,  $n_D = 1.4700$  at  $20^\circ\text{C}$ ,  $6.0 \mu\text{m}$  core radius). The mode cut-offs in this case are not marked by any appreciable drop in intensity, due to the fact that very little energy

was coupled into the higher order modes. Between 47 and 48°C the oscillations have a complex structure reminiscent of interference between 3 or more LP modes. The interfering modes in this region were identified as being  $LP_{01}$ ,  $LP_{11}$  and  $LP_{21}$ . The oscillations disappear at the  $LP_{11}$  modecut off, at about 51°C where only the fundamental  $LP_{01}$  mode is guided.

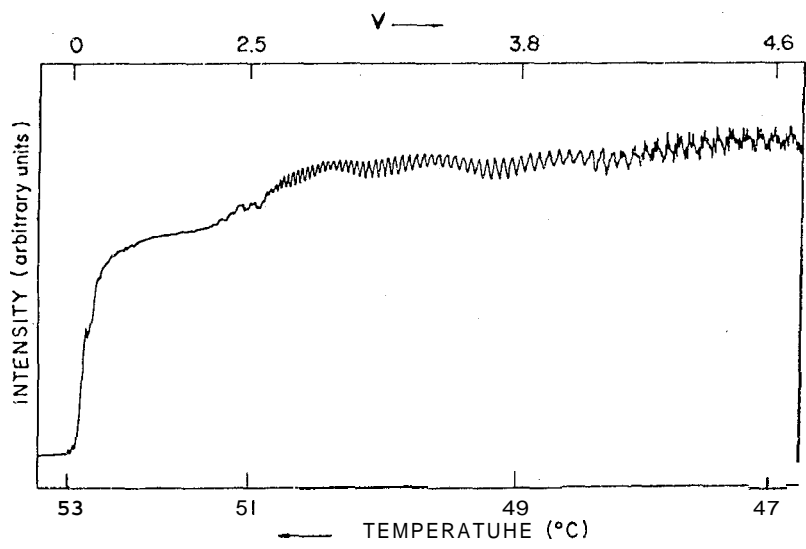


Fig.3 - Transmitted intensity as a function of temperature and v-value for fiber A.

Referring again to fig.2, we notice the lack of oscillations in the region below  $v=4$ . This is due to the fact that all light in the interfering modes falls on the detector. However, the amplitude of interference between modes may be enhanced by truncating the field pattern of the modes involved on the detector surface by placing a pinhole or other spatial filter in front of the detector, thus helping in precise measurement of the period of oscillations. On the other hand, this may complicate the interference of higher order modes. Figures 4 and 5 shows such an enhancement in Fibers B and C respectively. It can be clearly seen that, below 29°C, almost all the guided modes interfered causing a complex structure in the transmitted intensity pattern.

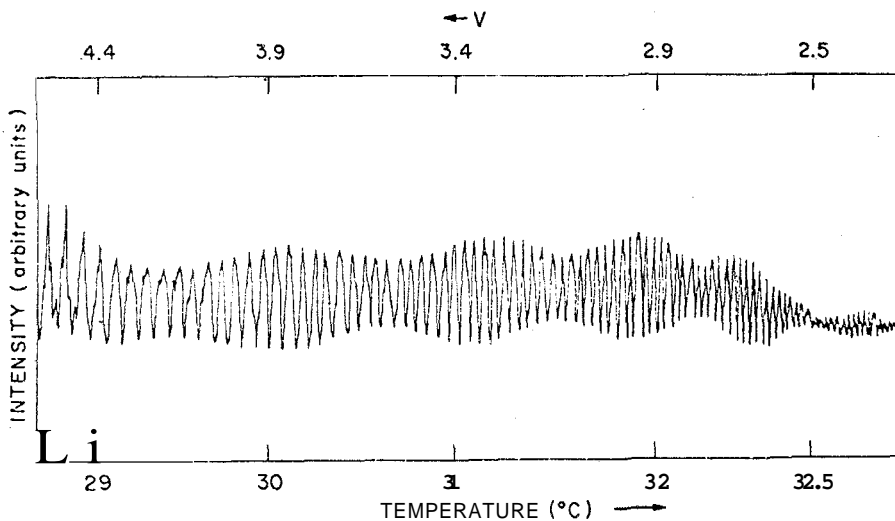


Fig.4 - Transmitted intensity of fiber B as a function of temperature and  $v$ -value with a pin-hole in front of the detector.

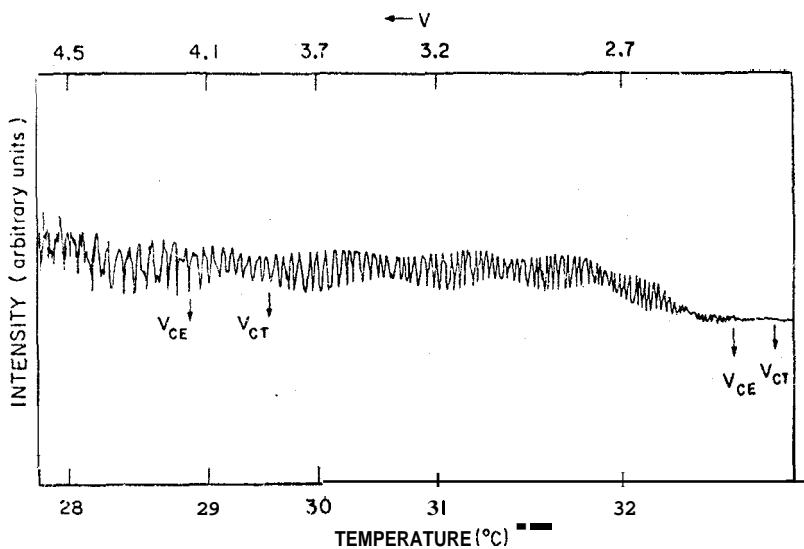


Fig.5 - Transmitted intensity as a function of temperature and  $v$ -value for fiber C, with a pin-hole in front of the detector.

#### 4. DISCUSSION

The experimental results show two types of oscillations, one with period  $\tau_1$ , ranging between 0.02 and 0.08° and another as beats of period  $\tau_2$ , ranging between 0.3° and 1.3°. We discuss below these oscillations and explain them on the basis of interference between LP mode groups and birefringence induced by core ellipticity.

##### A. Interference between different LP mode groups

As mentioned in section 3, it was not always possible to completely identify the set of modes which cause oscillations, particularly in the case of interference between higher order modes. In most cases, however, it was possible to identify visually at least one of the interfering mode groups without any ambiguity. The other one was then identified by comparison with theory. This was done in the following way: the normalized propagation constant  $b$  for the first five LP modes was calculated using Gloge's theory<sup>1</sup> and plotted vs  $v$  in the first part of this work<sup>3</sup>.

Using Gloge's theory, the normalized propagation constant  $b$  and the ratio of the power carried out in the core to the total power carried by each mode  $P_c/P_t$  were calculated for the first LP modes. In this way the period  $P$ , given by eq. (20) was calculated and plotted as a function of  $v$  (fig. 6) for distinct pairs of LP mode groups. The experimental values of periods for different fibers were shown for the LP modes in fig. 7.

The close agreement between the theoretical and experimental values seen here can therefore be used to identify which pair of mode group are involved in each interference pattern. Moreover, the best fit of the theoretical curve to the experimental data can be obtained by using the core radius as an adjustable parameter. This technique for determining the core radius of a hollow fiber is much more precise than optical microscopy. From the data, the core radius can be measured to a precision of better than 5%. This corresponds to a precision of 0.3  $\mu\text{m}$  in a typical case. However, in the case of fiber C, the core radius was measured with 0.1  $\mu\text{m}$  of precision.

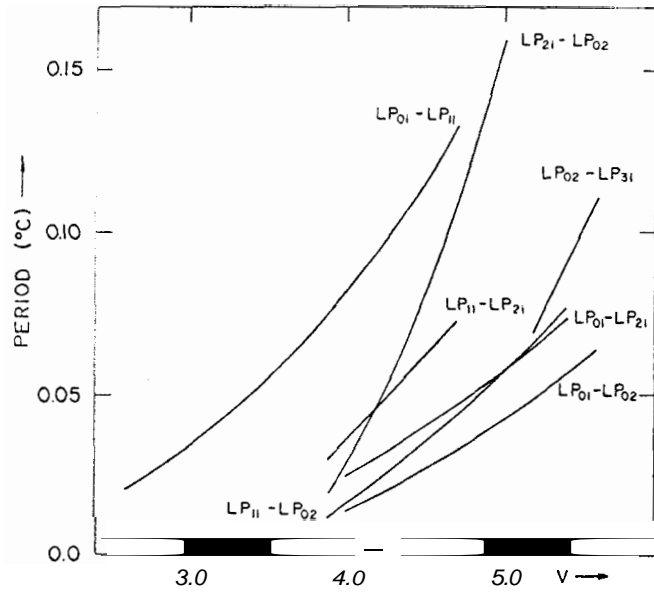


Fig.6 -  $v$ -dependence of the theoretical period due to interference between different pairs of LP mode groups.

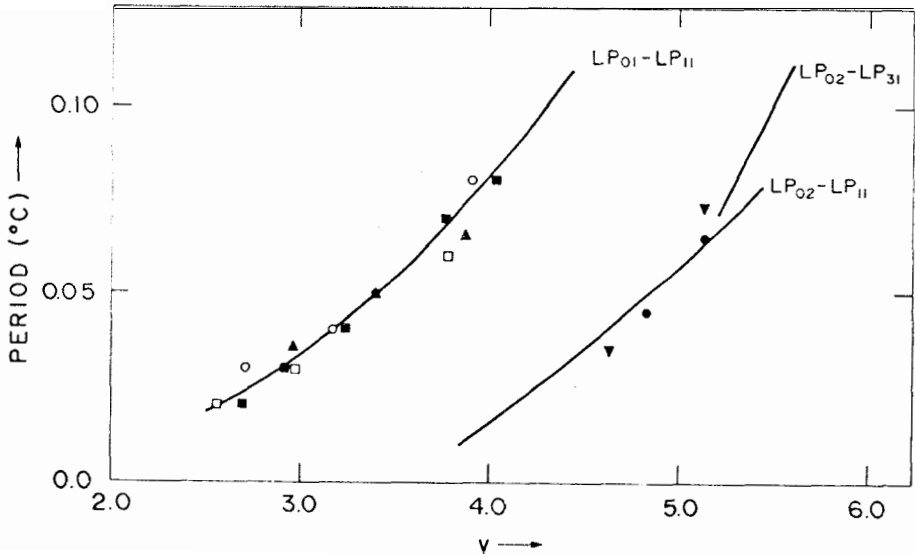


Fig.7 -  $v$ -dependence of theoretical (solid lines) and experimental (points) period:  $\Delta$  - fiber A;  $\circ$  - fiber B;  $\blacksquare$  - fiber C;  $\square$  - fiber F;  $\blacktriangledown$  - fiber D;  $\bullet$  - fiber E.

## B. Birefringence Induced Interference

Considering again the oscillations shown in figures (3,4,5) it is seen that a slow modulation of period ranging between 0.3 and  $1.3^\circ\text{C}$  appears in the region of  $2.4 < \nu < 3.8$ . On the other hand, no oscillation is observed in the region of single-mode propagation ( $\nu < 2.4$ ). In the presence of a small amount of core ellipticity, one would expect to see beating between the  $x^{LP_{01}}$  and  $y^{LP_{01}}$  modes. Furthermore, the modulation of a the beat pattern between 2.4 and 3.8  $\nu$ -values should be caused by interference between  $x^{LP_{01}}$ ,  $y^{LP_{01}}$ ,  $0^{LP_{11}}$  and  $e^{LP_{11}}$  modes.

Using eqs. (21) and (22) it is possible to explain why the beating of the fundamental  $LP_{01}$  mode is not observed. The former equation shows a dependence of the birefringence proportional to  $(\Delta)^{+3/2}$  and the latter proportional to  $(\Delta)^{+1/2}$ . As other terms are of approximately the same magnitude and since  $\Delta < 0.01$ , the birefringence due to core ellipticity in the fundamental mode is less than 1% that of the  $LP_{11}$  mode group. The period of oscillation predicted is thus much greater than the temperature interval over which the fiber is single mode. The period of the beating due to the difference between the propagation constants of the same LP mode groups ( $\beta_{HE} - \beta_{EH}$ ) was calculated using the Tjaden<sup>6</sup> approximation. The period which results is about ten times greater than the experimentally observed period. Therefore,  $(\beta_{HE} - \beta_{EH}) \ll (\beta_e - \beta_0)$ , and consequently in eq. (23),  $A \gg 1$  and the period can be calculated from the difference in  $\beta$ 's of the polarized modes.

Using eq. (30), a theoretical expression is obtained for the periods, which is shown in solid line in fig. 8. On the same graph are shown experimental values for the period, which are defined by the temperature difference between oscillation crests (i.e. between peak values of oscillation amplitudes) and the corresponding temperature was taken to be half-way between peaks. The theoretical curves were fitted by using the previously determined value of  $a$ , and then  $e$  was determined by the best Fit of the theory to the experimental data. We found typically  $e \approx 0.36$  for our samples, with an uncertainty due to the uncertainty in the core diameter ranging from  $\pm 0.01$  for fiber C, to  $\pm 0.03$  for fiber B. In addition, the scattering of period values caused a random error in  $C$  of the order of 2%.

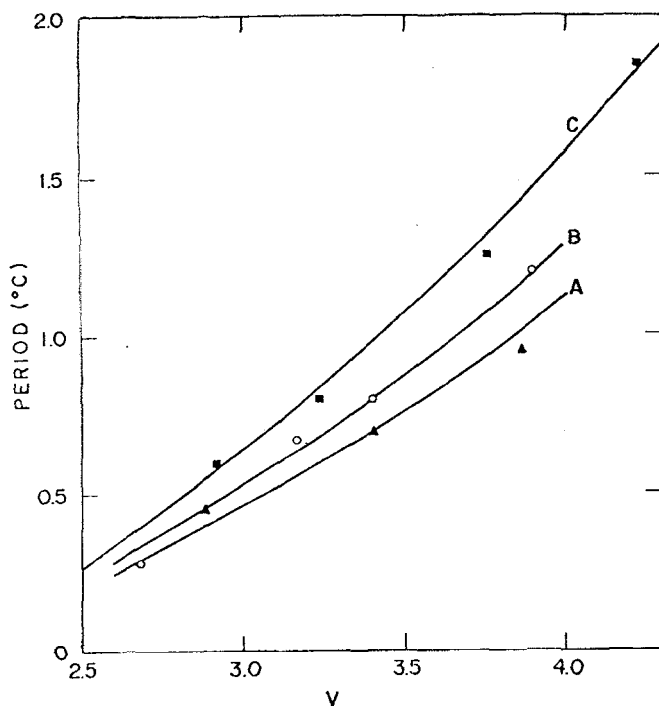


Fig.8 -  $V$ -dependence of the period due to ellipticity induced interference between  ${}_oLP_{11}$  and  ${}_eLP_{11}$  modes. The solid curves represent the theoretical values corresponding to experimental data for fiber A, B and C.

The length resolution of both types of measurement based on the maximum measurable beat period (which corresponds to approximately the distance between mode cut-offs) for our fibers, turned out to be less than 1 cm for the diameter measurement and about 10 cm for the ellipticity measurement.

One notices the excellent agreement between experiment and theory, which shows that the technique provides an accurate way of measuring core ellipticity of liquid core fibers.



## 5. CONCLUSION

We have used the large temperature dependence of the refractive index of LCFs to vary the number of modes in the fiber. We observed oscillations in the transmitted intensity caused by interference between modes which are characterized by two distinct periods. The theoretical interpretation allows identification of the modes involved and provides simultaneous measurement of core diameter and ellipticity to very high precision and in both the measurements can be performed on several LP mode groups, thereby offering a means of comparison and consistency check. This non-destructive technique of geometrical characterization can be extended to solid core fibers.

We acknowledge Telecomunicações Brasileiras S/A (Telebrás) for financial support and Profs. Hugo Fragnito e Alvin Kiel for many helpful discussions.

## REFERENCES

1. D.Gloge, *Applied Optics* 10, 2252 (1971).
2. Y.Murakami, A.Kawana and T.Tsuchiya, *Applied Optics* 18, 1101 (1979).
3. S.Planas, E.Bochove, R.Srívastava, *Rev. Bras. de Física*, 13(1), 55 (1983).
4. E.Snitzer and H.Oesterberg, *J.Opt.Am.* 51, 499 (1961).
5. A.Snyder and W.Young, *Journ. Opt. Soc. Am.*, 68, 297 (1978).
6. D.Tjaden, *Phillips J. of Research* 33, 103 (1978).

## Resumo

Foram observadas oscilações na intensidade transmitida em fibras de núcleo líquido como função da temperatura. As oscilações mais rápidas se interpretam como devidas à interferência entre vários grupos de modos da fibra circular. As variações mais lentas de períodos de uma ordem de magnitude maior são causadas por um batimento entre modos que pertencem ao mesmo grupo e que tem quebrado sua degenerescência devido à elipticidade do núcleo. Mostra-se que uma teoria simples concorda com os dados e tem sido aplicada para fazer medições de alta precisão não destrutivas, do raio e da elipticidade da fibra ao longo de seu comprimento.